

§15. Experimental Studies on the Neutron Emission Spectra and Activation Cross-section in IFMIF Accelerator Structural Elements

Itoga, T., Hagiwara, M., Baba, M., Oishi, T., Kamata, S. (Cyclotron and Radioisotope Center, Tohoku Univ.), Sugimoto, M. (JAERI), Muroga, T.

We have been conducting systematic experiments on the neutron emission spectrum and radioactivity accumulation in IFMIF structural elements in order to establish the data base for the design of IFMIF1,2). The experiments are carried out at the Tohoku University AVF cyclotron (K=110 MeV) facility. We measured neutron spectrum with the TOF method using a beam swinger system, and activation using a stack target technique.

Last year, we carried out new experiments for 40 MeV deuterons on Fe and Ta, and obtained the results of

- 1) neutron emission spectrum from a thick Fe, Ta target and
- 2) activation cross-sections of the $^{nat}\text{Fe}(d,x)^{51}\text{Cr}$, ^{52}Mn , ^{56}Co , ^{57}Co , and ^{58}Co reactions.

- 3) neutron emission spectrum from a thin lithium target bombarded with 25 MeV deuterons, were also measured.

The experimental method was almost the same with previous experiments1,2) and described only briefly here.

A deuteron beam from the Tohoku University cyclotron was transported to the target chamber at the center of the beam swinger system in the No.5 target room. The neutron spectrum was obtained by using two NE213 scintillators, 14-cm-diam and 10-cm-thick, and 5-cm-diam and 5-cm-thick equipped with n- γ discriminators. The smaller one measured low energy region, and the larger one higher energy region. The data were accumulated as three-parameter data for TOF, n- γ spectra and pulse-height of the NE213 detector. The detection efficiency was obtained by calculation using the code SCINFUL-R.

We measured the activities in the targets after irradiation using high-pure Ge detectors by detecting the corresponding gamma-rays due to the decay of radioactive nuclides accumulated by the deuteron bombardment.

Thirty thin targets of carbon and aluminum with natural composition and 200- μm -thick were stacked to stop the incident beam in the targets. The targets were set on a remotely-controlled target changer together with a beam viewer.

The beam current was around a few nano-amps or less. A secondary electron suppressor was placed around the target. The beam charge on the target was measured with an ORTEC current digitizer and a multi-channel scaler to record the time history of the beam.

Figures 1 and 2 show thick target neutron emission spectrum from iron and tantalum, respectively, as a function of emission angle. Neutron spectra are measured over the almost entire range of secondary energies. They consist of two components: one is due to breakup of incident deuterons around 15 MeV with very strong angular dependence, and a

low energy component due to the evaporation and almost isotropic. The intensity of low energy component seems increasing with the target mass compared with the data on carbon and aluminum. Inversely, the breakup neutrons around 15 MeV looks to become less with the target mass. This result suggests that the breakup of incident deuterons is more dominant in light nuclides. Experimental neutron emission data covering the low energy region as the present data are very few and then the present can be used for the model development of the neutron emission.

In Fig.3-6, the results of the activation cross-sections are shown, together with other experiments. The present values for iron are consistent with other data. The present data can be directly used for estimation of radioactivity induced in the target and structural elements in IFMIF accelerator system.

Reference

- 1) T. Aoki et al., *J. Nucl. Sci. Technol.*, **41** (2004), 399-405
- 2) M., Hagiwara, et al., *J. Nucl. Materials*, **329-333**, (2004) 218-222

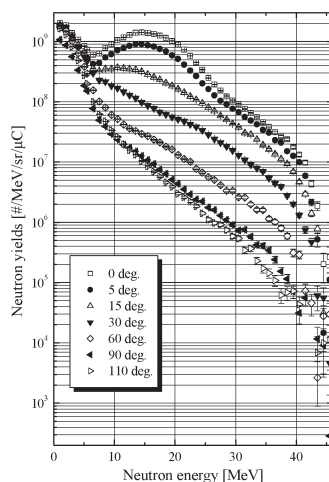


Fig.1 Thick target Fe(d,n) spectrum.

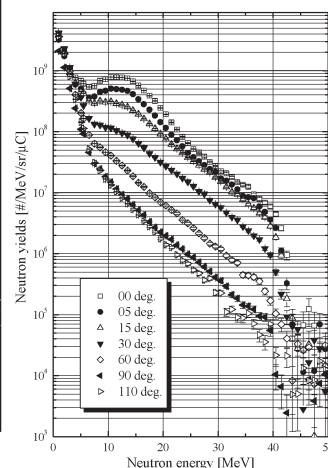


Fig.2 Thick target Ta(d,n) spectrum.

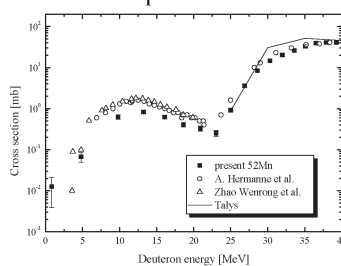


Fig.3 Fe(d,x) ^{52}Mn cross section

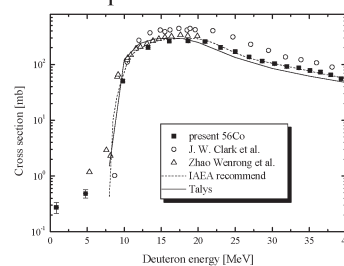


Fig.4 Fe(d,x) ^{56}Co cross section

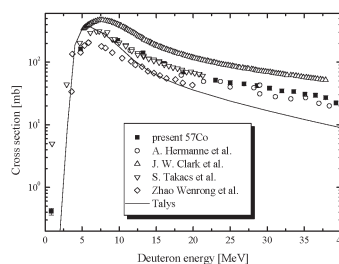


Fig.5 Fe(d,x) ^{57}Co cross section

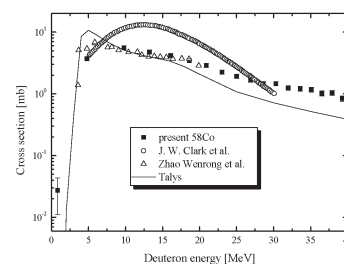


Fig.6 Fe(d,x) ^{58}Co cross section